Hydrological tracers for assessing transport and dissipation processes of pesticides in a model constructed wetland system

Elena Fernández-Pascual [1], Marcus Bork [1,2], Birte Hensen [3], Jens Lange [1]

[1] Hydrology, Faculty of Environment and Natural Resources, University of Freiburg, Freiburg, Germany
[2] Soil Ecology, Faculty of Environment and Natural Resources, University of Freiburg, Freiburg, Germany
[3] Institute of Sustainable and Environmental Chemistry, Leuphana University Lüneburg, Lüneburg, Germany

Correspondence to: Elena Fernández-Pascual (elena.fernandez@hydrology.uni-freiburg.de)

Abstract. Hydrological tracers have been recently used as a low-cost approach to study the fate and transport of pesticides in constructed wetlands. Yet, internal temporal and spatial mechanisms that dominate their transport and dissipation in such environments are still not fully understood. We have applied three tracers with different sorptive and reactive properties: bromide (Br), uranine (UR) and sulforhodamine B (SRB) to investigate dominant temporal and spatial transport and dissipation processes of three selected pesticides: boscalid, penconazole and metazachlor in a model constructed wetland system designed to perform high vertical-resolution sampling and monitoring on a long-term basis. The experimental observations revealed that two different preferential flow paths developed, one due to the constructional design of the inflow and the other one due to the influence of the free water at the surface along with the plants. Transport of solutes was driven by the injections and dominated for Br, UR and metazachlor. The final mass balance highlighted that the main dissipation pathways were sorption, transformation and plant uptake. Sorption was detected immediately after the injection of solutes, while transformation was enhanced by the presence of plants and the promotion of aerobic conditions. The detection of metazachlor transformation products confirmed the contribution of transformation to metazachlor dissipation, whereas boscalid and penconazole mainly experienced sorption processes. The use of hydrological tracers together with selected pesticides and coupled with high vertical-resolution sampling and monitoring proved to provide valuable information about transport vectors and dissipation processes of pesticides in a vegetated redox-dynamic environment on a long-term basis and detailed spatial scale.

1 Introduction

Pesticides are widely used to protect crops and increase their yields around the world. It is well known that their use might result in ecotoxicological effects in non-target environments (Stehle and Schulz, 2015a). Chemical analysis performed in the waters of European countries revealed that pesticides are often detected in surface waters (Müller et al., 2002). This problem becomes even more severe when the pesticides produce a variety of transformation products (TPs), whose toxicity or persistence is unknown. In fact, the presence of TPs in water bodies has also been reported in numerous studies (Kolpin et al., 2004; Eurostat, 2012; Reemtsma et al., 2013).

Buffer zones emerged as a measure for controlling water pollution. Constructed wetlands are one example of buffer zones, where the removal of pesticides takes place. Indeed, constructed wetlands are designed to simulate and take advantage of processes that occur in natural wetlands (Vymazal et al., 2005), such as sedimentation, photolysis, hydrolysis, adsorption, microbial degradation and plant uptake (Vymazal et al., 2015). In these systems vegetation plays an essential role promoting sedimentation by reducing the current velocities of the water (Petticrew and Kalff, 1992), providing a substrate for microorganism in the roots and rhizomes (Hofmann, 1986) and creating oxidized conditions in the roots that stimulate aerobic decomposition (Brix, 1997). Removal processes in constructed wetlands may also be promoted through intermittent water flows by enhancing aeration and by providing different redox conditions suitable for the growth of different microbiological communities (Ong et al., 2010; Maillard et al., 2011; Fan et al., 2013).

The mitigation capacities of buffer zones have recently been studied by using hydrological tracers as a low-cost approach. Indeed, several studies have investigated transport and dissipation of pesticides in wetlands (Passeport et al., 2010; Lange et

al., 2011; Durst et al., 2013; Maillard et al., 2016) and farm ditches (Dollinger et al., 2017). Yet, most studies have treated the systems as black boxes and the time scales were typically limited to the time spans of the tracers breakthroughs at the systems outlet. Hence, internal temporal and spatial mechanisms that dominate pesticides transport and dissipation in buffer zones are still not fully clear, especially when it comes to different redox regimes, long time scales and the presence of vegetation.

5 Therefore, the objectives of this study are i) to identify temporal and spatial transport and dissipation processes in a model constructed wetland system by applying a multi-tracer approach together with high vertical-resolution sampling and monitoring on a long-term basis; ii) to compare the temporal and spatial behavior of the applied tracers with three pesticides selected as test substances and evaluate their main dissipation pathways; and iii) to assess the influence of vegetation and the alternation of different hydrologic conditions (saturated and unsaturated) on transport and dissipation processes.

10 The present experiment was conducted in a model constructed wetland system with one half planted with two common wetland plants and the other half unplanted (control). The constructed wetland was equipped with a system designed to perform high vertical-resolution sampling and monitoring on a long-term basis. Three hydrological tracers were chosen as reference substances according to their reactive nature: bromide (Br) as a non-adsorbing tracer (Whitmer et al., 2000), uranine (UR) as a photosensitive tracer (Gutowski et al., 2015) that can undergo processes of (bio-) chemical transformation (Lange et al., 2018)

15 and sulforhodamine B (SRB) as a highly sorptive tracer (Kasnavia et al., 1999). Whereas, three commonly applied pesticides with different physicochemical properties were selected as test substances: boscalid (2-chloro-N-(4'-chlorobiphenyl-2-yl) nicotinamide), penconazole ((RS)-1-[2-(2,4-dichlorophenyl) pentyl]-1H-1,2,4-triazole), and metazachlor (2-chloro-N-(pyrazol-1-ylmethyl) acet-2',6'-xylidide).

2 Materials and Methods

2.1 Chemicals

20 The physio-chemical properties of tracers and pesticides are summarized in Table 1. UR was purchased from Simon & Werner GmbH (CAS-no. 518-47-8), SRB from Waldeck GmbH & Co KG (CAS-no. 3520-42-1) and Br was obtained as sodium bromide from Carl Roth GmbH & Co KG. Boscalid (99.8%), penconazole (99%) and metazachlor (99.7%) already dissolved in acetonitrile (99.9%) were purchased from Neochema (Bodenheim, Germany). The analytical standards of boscalid (99.9 %),

25 penconazol (99.1 %), metazachlor (99.6 %) and p-Chlorobenzoic acid (99%) were purchased from Sigma-Aldrich Chemie GmbH (Steinheim, Germany). 1,2,4-Triazole (99.5%) was purchased from LGC Standards (Wesel, Germany). Metazachlor-ESA (95 %) and metazachlor-OA (98.8 %), hereunder named as met-ESA and met-OA, respectively, and the internal standard Terbutryn-D5 (98.5 %) already dissolved in acetonitrile (100 µg mL-1) were received from Neochema (Bodenheim, Germany).

The target injection masses of tracers and pesticides for an injection volume of 40 L were calculated according to Durst et al.

30 (2013). Standard stock solutions of 1 g L^{-1} for UR and SRB and of 10 g L^{-1} for Br were prepared in MilliQ water. Pesticides (0.1 g L^{-1}) dissolved in acetonitrile were directly mixed with the injection solution. The concentration of tracers and pesticides in the injection solution was 100 mg L, 50 µg L^{-1} and 100 µg L^{-1}, for sodium bromide, UR and SRB, respectively; and 50 µg L^{-1} for boscalid, penconazole and metazachlor.

2.2 Design of the model constructed wetland system

35 The model constructed wetland system consisted of a glass tank 177.4 cm long, 47.6 cm wide and 56.8 cm deep (Fig. 1). The system was divided into three parts, two of them inlet and outlet reservoirs located at both ends and separated by two glass walls and a third part located in the middle consisting of the main bed of sediments. The bottom was filled with 10 cm of gravel (grain size 4-8 mm) and topped with 32 cm of sand (grain size 0.01-2 mm). The characteristics of the system are given in Table 2A. One half of the system was left unplanted (control), while the other half was planted with two species of widespread and

40 ubiquitous wetland plants (*Typha latifolia* and *Phragmites australis*) that were purchased from a local garden center with an

average initial height of 79.8 cm ± 18.6 and 76.9 cm ± 10.1, respectively. The whole experiment was carried out indoors in a laboratory assembly, therefore 64 OSRAM SSL 3W light-emitting diode lamps for plant growth (Purple Alien 2.0, LED Grow Shop, Germany) were installed with daily photoperiods of 11 hours.

The inlet and outlet were intended to create vertical water flows. This was achieved through the installation of two pairs of peristaltic pumps coupled to Plexiglas pipes (15 mm diameter) that were connected to the bottom of the system; and another two pairs of peristaltic pumps coupled to Plexiglas pipes that channelled directly into the inlet and outlet reservoirs, respectively. A tank with a capacity of 350 L that was connected to the tap water served as external inlet reservoir, while a second tank with a capacity of 1000 L received the waste water. In order to monitor the water level, three pairs of PVC observation pipes (DN: 35-40 mm, STÜWA Konrad Stükerjürgen GmbH, Germany) with a length of 50 cm, were arranged symmetrically on both sides at the center line of the system. One half of the pipes were located at the gravel layer and the other half in the sand.

With a view to obtaining pore water samples at a high vertical resolution, a multi-level pipe was designed with a sampling resolution of 12 cm. This created a total of four sampling depths that ranged from the gravel to the uppermost layer of the sand. Two multi-level pipes were installed in the sediment bed, one at the non-vegetated and the other one at the vegetated half of the system. Small glassfilters (12.5 mm diameter, porosity 2, ROBU, Germany) were installed in both multi-level pipes at each sampling depth. The filters were connected to a multichannel peristaltic pump (Pulse-free flow peristaltic pump, Gilson, France) via capillaries made of stainless steel (1/16" inner diameter, Swagelok, Germany) that were directly inserted into TYGON tubes (ID: 1.02 mm, Proliquid, Germany). In addition, 5TE sensors (Decagon Em50 serie, Campbell Scientific) and redox probes (Paleo terra, Amsterdam, The Netherlands) were installed at the same depths in both multi-level pipes. Glassfilters, sensors and probes were separated from each other at an angle of 90 degrees at each sampling depth (Fig. 1B). Furthermore, a reference electrode (Ag:AgCl) connected to the redox probes, was inserted in the sediment between the multi-level pipes. All sensors and probes were connected to a datalogger (CR1000, Campbell Scientific).

2.3 Operation of the model constructed wetland system

The model constructed wetland system was designed to alternate saturated with unsaturated conditions (long periods of aeration). In total three phases were created (Fig. 2): 1) saturation with target substances (one week), 2) drying by evapotranspiration (three weeks) and 3) saturation with clean water (one month). The saturation phases were preceded by the injection of solutes or clean water (tap water). The operation of the constructed wetland is summarized in Table 2B. Prior to the injection of tracers and pesticides, the system was drained until field capacity was reached. The whole experiment lasted seven months (from March 2017 to October 2017), during which two identical experimental runs were performed. The first run (from March 9 to May 9, 2017) was followed by a resting period of about three months (from May 9 to August 1, 2017), during which occasional water additions to maintain the vegetation were carried out. After this, the second run (from August 1 to October 3, 2017) was conducted.

The execution of the injections is shown in Fig. 3. Three injections took place in each run of the experiment: (i) initial surface injection of tracers and pesticides, (ii) injection of clean water (tap water) from the bottom of the system and (iii) flushing of the sediments with clean water from the bottom. The surface injection (i) was performed after having drained the system. The solution was constantly pumped into the inlet reservoir. Then, it began to overflow the inlet reservoir and enter the sediments bed in descending direction. As the inflow progressed, the solution extended to the rest of the sediments in an upward direction. The inflow was maintained until the system became saturated and a surface layer of approximately two centimeters height was formed on top of the sediments. The second injection (ii) was performed at the end of the drying phase by pumping clean water (tap water) from the bottom. The water flowed evenly through the sediment in vertical upward direction. The inflow was maintained until the system became saturated and a surface layer of approximately two centimeters height was formed on top of the sediment. This injection was repeated throughout the second saturation phase in order to keep the system constantly saturated. The flushing of the system (iii) was performed at the end of the second saturation phase and it was intended to recover

all mobile fractions of the target compounds. To do this, clean water (tap water) was injected from the bottom and was allowed to flow into the system continuously. Water overflowed the main bed and exited towards the outlet reservoir, from where it was pumped to the waste tank.

2.4 Sampling and monitoring

5   Pore water samples were collected from different depths twice a week during the experimental runs. The sampling of pore water was performed simultaneously in order to prevent mixing of waters. A volume of 60 mL of pore water was transferred to 100 mL brown glass bottles and stored at 4°C for major ions and tracers analysis. Previously, a volume of 10 mL was transferred to 15 mL Polypropylene tubes and stored at -20°C for the subsequent pesticide and TPs analysis. Additional pore water samples were taken before and after the initial injections of tracers and pesticides to account for the background. During

10 the flushing of the system, surface water samples were collected at the outlet and transferred to 100 mL brown glass bottles. Following this, the samples were stored at 4 or -20°C depending on the type of analysis performed afterwards (major ions and tracers analysis or pesticide and TPs, respectively).

At the end of the experiment, the sediment bed was emptied of its gravitational water. Following this, 16 sediment cores (four per longitudinal and four per lateral transect) were collected by inserting plastic pipes into the sediment. Sediment cores were

15 divided into four fractions, each representing a different sampling depth (0-8 cm, 9-20 cm, 21-32 cm, 33-42 cm). The sediment samples were dried at room temperature for 24 h and stored in the dark for subsequent measurements of tracers, total organic carbon and iron oxides. Then, the plants were removed from the vegetated zone and separated into aerial parts (stems and leaves) and roots. Immediately after they were oven dried at 60°C for approximately 24 hours and stored in the dark for subsequent measurements of tracers. Biomass was determined on a dry matter basis.

20 Temperature, soil moisture, conductivity and redox potential were constantly monitored by means of the datalogger with an interval of two minutes throughout the entire experiment. Redox potential was calculated by adding the potential from the reference electrode (Ag/AgCl) to the measured potential (Vorenhout et al., 2011). The final result was corrected for differences in temperature according to Bard et al. (2018).

2.5 Laboratory analysis

25 #### 2.5.1 Major ions and tracers in the pore- and outlet-water

Pore- and outlet-water samples were measured for major ions (Na^+, NH_4^+, K^+, Ca^{2+}, Mg^{2+}, Br^-, SO_4^{2-}, Cl^-, NO_3^- and NO_2^-) by ion chromatography (Dionex ICS-1100, Thermo Scientific, USA). All samples were previously filtered with a 0.45 µm filter.

Concentrations of the tracers UR and SRB in pore and outlet water samples were measured by fluorescence spectrometry (Perkin Elmer LS 50 B) as previously described (Leibundgut et al., 2009). Briefly, a synchronous scan method was applied

30 with an excitation/emission wavelength difference of 25 nm and target wavelengths of 488 nm and 561 nm for UR and SRB, respectively. Detection limits were 0.05 µg L^{-1} for UR and 0.1 µg L^{-1} for SRB.

2.5.2 Pesticides and TPs in the pore- and outlet- water

Pore- and outlet-water samples were analyzed for the pesticides boscalid, penconazole, metazachlor and their known TPs (metazachlor-ESA and -OA, p-Chlorobenzoic acid (boscalid), and 1,2,4-Triazole (penconazole)). Acetonitrile (LC-MS grade;

35 VWR International GmbH, Darmstadt, Germany) was used as organic mobile phase in chromatography and for the preparation of stock solutions. Aqueous mobile phase was prepared with ultrapure water (Membra Pure, Germany; Q1:16.6 MΩ and Q2: 18.2 MΩ). Samples were filtered using syringe filter units (CHROMAFIL® Xtra RC-20/25; Macharey-Nagel, GmbH & Co. KG, Germany). Each sample (990 µL) was spiked with 10 µL Terbutryn-D5 as internal standard. Analysis of 5 µL of each sample was done by LC-MS/MS (Agilent Technologies, 1200 Infinity LC-System and 6430 Triple Quad, Waldbronn,

Germany). Mobile phases were 0.01 % formic acid (A) and acetonitrile (B) with a flow of 0.4 mL min⁻¹. Gradient was as follows: 0-1 min (10% B), 1-11 min (10-50% B), 11-18 min (50-85% B), 18-21 min (85-90% B), 21-24 min (90% B), 24-26 min (90-10% B) and 26-30 (10% B). A NUCLEODUR® RP-C18 (125/2; 100-3 µm C18 ec) column (Macherey Nagel, Düren, Germany) was used as stationary phase with a set oven temperature of T = 30°C. Limits of detection (LOD) and quantitation

5   (LOQ) were calculated with DINTEST (2003) according to DIN 32645.

2.5.3 Extraction and measurement of tracers in the sediments and plants

UR and SRB in the sediment (sand) and plants were extracted as described by Wernli (2011). In brief, two grams of the dried material were mixed with 10 mL of ammonia-ethanol solution (40:60, v/v). Dried stems, leaves and roots were previously grinded with a vibratory disc mill (Siebtechnik GmbH, Germany). All samples were shaken on an IKA HS 250 reciprocating

10   shaker for 30 minutes at 240 rpm and stored at 4°C in the refrigerator for at least 24 hours. Afterwards, supernatant was collected, filtered (< 0.45 µm) and measured for the tracers. The resulted curves were corrected through interpolation and subtraction of the background signal from the peak intensity as described by Leibundgut et al. (2009).

A different methodology based on McMahon et al. (2003) was used to measure Br in the sediment (sand) and plants to avoid the interference of the ammonia-ethanol solution with the ion chromatograph. Samples were prepared in the same way as

15   previously described, but they were mixed with 20 mL of deionized water instead. Following this, they were shaken on an IKA HS 250 reciprocating shaker for 1 hour at 240 rpm and later centrifuged at 3000 rpm for 30 minutes (Megafuge 1.0R; Heraeus Instruments). Supernatant was then taken, filtered (< 0.45 µm) and measured by ion chromatography (Dionex ICS-1100, Thermo Scientific, USA).

2.5.4 TOC and iron oxides in the sediment

20   Total organic carbon (TOC) was measured in the sediment (sand) with a CNS-analyser (Vario El Cube, Elementar, Germany) after grinding the dried samples with a vibratory disc mill (Siebtechnik GmbH, Germany). Dithionite-extractable Fe (Fe_d) in the sediment (sand) was extracted according to Mehra and Jackson (1960) and measured using inductively coupled plasma - optical emission spectrometry (Spectro Ciros CCD, Spectro Analytical Instruments GmbH, Germany).

2.6 Data Analysis

25   Spatial and temporal dynamics of transport and dissipation of solutes were studied by analysing their breakthrough curves obtained in the pore water at different depths. The influence of the vegetation and the hydrologic conditions were evaluated by comparing the results of the vegetated with the non-vegetated zones and the results of the saturation with the drying phases. The performance of the two experimental runs was evaluated by means of the correlation between the Br breakthrough curves of the first and the second run. In addition, transport and plant uptake were assessed with the total percentage of Br recovered

30   from the pore water of each experimental run. Here, a distinction between the different zones and depths was made.

The general behavior of the solutes and their relationship in the pore water throughout the experiment were analyzed by correlation matrices. Spearman rank correlation coefficients (rho_s) were applied since the data did not fit a normal distribution. Correlations were calculated individually for the vegetated, the non-vegetated zone and the different depths. Additionally, the predominance of transport processes in the pore water was examined by looking at the correlation between the solutes and Br.

35   Here, a strong correlation with Br was assumed to be due to a prevalence of transport over other processes in the pore water, given the most conservative character of Br.

Further comparisons between tracers, pesticides and their TPs were made by analyzing their cumulative recovery curves obtained at the outlet after the flushing phases. The fate of the solutes and their main dissipation pathways were analyzed with a final overall mass balance that accounted for five different compartments (pore water, outlet water, sediments, stems + leaves

40   and roots). The mass of tracers and pesticides recovered in the pore water was calculated as the sum of the weekly dissolved

concentrations multiplied by the volume sampled. The mass of tracers and pesticides recovered in the outlet water was calculated based on the recovery curves obtained during the flushing phases. The mass of tracers and pesticides recovered in the sediments and plants was determined as the concentrations measured in their corresponding compartments multiplied by the total amount of sediments and plants in the system, respectively.

5 In the present study the pesticides and their TPs could only be measured in the pore water and the outlet water. Statements on their behaviour in the remaining compartments were made according to their physicochemical properties, the results of the breakthrough and recovery curves, their comparison with the tracers and the findings of similar studies reported in the literature.

3 Results and discussion

3.1 Breakthrough curves of solutes in the pore water

10 Early breakthrough peaks of tracers and pesticides (Fig. 4) were reached in the non-vegetated zone (represented by solid lines) of the lowermost layer (39 cm) after the surface injection. By contrast, in the vegetated zone of the same layer (represented by dashed lines) only low relative concentrations of Br, UR and metazachlor could be detected. Similar early breakthrough peaks were reached in the vegetated part of the uppermost layer (3 cm), although the tracers and pesticides displayed more than double the relative concentration measured in the lowermost layer. Conversely, in the non-vegetated part of the uppermost layer, the

15 tracers and pesticides showed a delayed breakthrough peak with lower relative concentrations.

In the following days, two of the major metabolites of metazachlor (met-ESA and met-OA) were detected in the uppermost layer. In the vegetated zone, met-ESA peaked first (day 6). Five days later met-ESA appeared in the non-vegetated zone of the same layer with half of the relative concentration that was measured in the vegetated zone. Yet, during the same phase of the second run no TPs were found. A second peak of both met-ESA and met-OA, with about double the relative concentration

20 measured before, was observed in the vegetated uppermost layer 32 days after the initial injection during the first run. Whereas in the same period of the second run only met-ESA peaked displaying residual amounts.

A delay of about one month in the breakthrough peaks during both runs was observed in the middle sediment layers (15 and 27 cm). The maximum relative concentrations were reached at the end of the drying phase. This was related to the possible migration of solutes during the drop in the water table from the surface to lower layers. In this case, while in the non-vegetated

25 zone clear breakthrough peaks of Br, UR and metazachlor could be detected, in the vegetated zone only Br displayed observable amounts. Yet, a clear breakthrough peak of Br could only be measured during the second run at the sampling depth of 27 cm.

The relative concentration of tracers and pesticides experienced an overall decline during the second saturation phase until the end of the experiment in both runs. However, a late second peak of Br, UR and metazachlor was observed in the non-vegetated part of the uppermost layer during the second run. This result was related with possible upward migration of solutes from lower

30 layers during the injection of clean water from the bottom.

3.1.1 Spatial and temporal dynamics of transport and dissipation processes

From a spatial point of view, both the lower- and the uppermost layers were affected by preferential flow paths, as evidenced by the measurement of early breakthrough peaks of tracers and pesticides. The constructional design of the inflow most likely influenced the transport of solutes causing preferential flow towards the bottom. In addition, the free water at the surface and

35 the channeling effect of the vegetation caused preferential flow paths towards the surface, similar to the findings of Durst et al., 2013. This was corroborated by the highest relative concentrations of tracers and pesticides measured in the vegetated zone of the uppermost layer. In the middle layers, the dominant processes differed between zones as evidenced by the different redox potentials measured in the vegetated and the non-vegetated zone. In this case, transport from the upper layers dominated in the non-vegetated zone, as confirmed by the delayed breakthrough peaks. Conversely, plant uptake, mineralization in the roots and

40 sorption processes possibly played major roles in the vegetated zone, since overall small amounts of Br were measured.

The uppermost layer was also a hot spot for sorption and degradation processes, regardless of the presence of vegetation. This conclusion is based on the fact that the most sorptive solutes (boscalid and penconazole) did not migrate to lower layers during the drop of the water table. Besides, the TPs of metazachlor were only detected in the uppermost layer.

From a temporal point of view, preferential flow took place at the beginning of the experiment according to the early breakthrough peaks detected. Later, vertical transport processes dominated during the drying phase, as demonstrated by the temporal dynamics of the most mobile solutes (Br, UR and metazachlor). Sorption most likely ocurred shortly after the injection of tracers and pesticides, since the relative concentration of the most sorptive solutes decreased rapidly in the areas where they were detected. Likewise, degradation processes were observed at early stages and dominated during the drying period, when the maximum relative concentration of metazachlor TPs were measured.

3.1.2 Role of vegetation and hydrologic conditions in transport and dissipation processes

The overall absence of breakthrough curves in the vegetated zone of the middle layers and the early breakthrough curves measured in the vegetated zone of the uppermost layer confirmed the influence of the plants, in both, dissipation processes and the promotion of preferential flows, respectively. In addition, the increased occurrence of metazachlor TPs in the vegetated zone of the uppermost layer evidenced the role of the plants in enhancing transformation processes.

The performance of the system over time in terms of transport and dissipation was also affected by the presence of plants. When comparing the correlation between the breakthrough curves of Br (chosen for its most conservative character) of the first and the second run, differences between the vegetated and non-vegetated zones were observed (Table 3). Indeed, with the exception of the uppermost layer, the non-vegetated zone showed strong correlation between the two runs regardless of the layer, whereas the vegetated did not show any correlation. This means that the performance of the non-vegetated zone was similar in both runs, whereas the vegetated behaved differently. We hypothesize that possible changes in root density and/or spatial distribution occurred during the experiment. This assumption was supported by visual observations of the root system in the sediment (Fig. 5). As a result, presumably both transport processes and plant uptake varied over time (Goss et al., 1993). The magnitude of these changes was analyzed by the total percentage of bromide recovered from the pore water (Table 4). Here, similar values were observed in both runs for the vegetated zone at 39 and 27 cm depth. Consequently, the different breakthrough curves measured in each run was most likely due to changes in transport processes rather than plant uptake. In contrast, the vegetated part at 15 cm depth showed different Br recoveries between the two runs. Therefore, plant uptake was probably more important than transport in this layer. The uppermost layer also displayed different Br recoveries in the vegetated zone, but in this case given that no correlation was found between the first and the second run, the differences were most likely due to the strong influence of preferential flow.

The results of the breakthrough curves also revealed that the alternation of different hydrologic conditions (saturation with drying periods) enhanced transformation processes, as already reported in other studies (Vymazal et al., 2015; Maillard et al., 2016). Indeed, the maximum relative concentration of metazachlor TPs were measured after the promotion of aerobic conditions during the drying period.

3.2 Relationship between solutes throughout the experiment

Two layers exhibited the strongest correlations between solutes (Fig. 6): the lower- and the uppermost layer. These findings were consistent with the hypothesis that transport by preferential flow was the dominant process in these layers, given the strong correlation shown between the solutes and Br. Yet, this was not true for all pesticides, as boscalid and penconazole did

not correlate with Br in the vegetated zone of the lowermost layer and the non-vegetated zone of the uppermost layer. For these pesticides, probably other processes, such as sorption or plant uptake dominated during the experiment.

In the middle layers only UR and metazachlor exhibited significant correlations with Br, although in the vegetated zone no correlation was found between metazachlor and Br. These results suggested that transport was the dominant process for

5 metazachlor in the absence of vegetation, while in the vegetated zone other processes, most likely plant uptake, mineralization in the roots, sorption and transformation predominated. In contrast, UR correlated with Br in all layers regardless of the presence of vegetation. Therefore, transport was almost certainly the dominant process for UR in the pore water during the experiment. This was not the case for SRB, whose strong positive correlation with Br in the upper- and lowermost layers further confirmed the creation of preferential flow paths, given its strong sorptive character.

10 As for the TPs of metazachlor, Met-ESA, displayed strong positive correlation with the tracers and pesticides in the vegetated zone of the uppermost layer, whereas met-OA did not show any statistically significant correlation. These results may indicate that met-ESA experienced transport processes in the uppermost layer after it was formed in the system. Yet, for met-OA no conclusion could be drawn, given the lower amounts detected in the present study.

3.3 Recoveries of solutes at the outlet

15 The results of the cumulative recovery curves obtained at the outlet during the first flushings (Fig. 7) showed a rapid increase in accumulated mass recovery for Br, whereas the rest of the solutes displayed comparatively slower increases. In the following flushings, the accumulated mass recovery of SRB, penconazole and boscalid gradually increased, while for Br, UR and metazachlor it stabilized. These results suggested that the retained fractions of SRB, boscalid and penconazole in the soil were greater than for Br, UR and metazachlor. Indeed, SRB, boscalid and penconazole still exhibited increases in their accumulated

20 mass recoveries weeks or even months after the first flushing. Analogous recovery curves for SRB, boscalid and penconazole were observed (Fig. 7-A1 and B1) even though SRB has different chemical properties and showed higher mass recoveries than boscalid and penconazole (Table 5). Yet, this was only true after the system was repeatedly flushed. A possible explanation for these similarities is that SRB, boscalid and penconazole have high K_{oc} values, which means that these compounds are strongly retained in the soil matrix (Long et al., 2005; Vallée et al., 2014; Dollinger et al., 2017).

25 Small amounts of metazachlor TPs, especially met-ESA, were also recovered at the outlet of the system, thereby evidencing their great mobility and persistence in the environment (Mamy et al., 2005; European Food Safety Authority (EFSA), 2008).

According to the total amount of tracers and pesticides recovered at the outlet after the flushings (Table 5), the tracers and pesticides were classified as follows: Br >> SRB >> UR >> Boscalid >> Penconazole >> Metazachlor. It is believed that several processes in our system, mostly adsorption by substrates, transformation and plant uptake, were responsible for the removal of

30 tracers and pesticides. Nevertheless, the physico-chemical properties of the compounds have been the determining factor for their dissipation. In this regard, Vallée et al. (2014) found that a greater retention of pesticides in the soil was related to higher hydrophobic properties (low solubilities and high K_{oc} values). Based on this assumption, we would have expected higher recoveries for metazachlor than for penconazole and boscalid, given its less hydrophobic character. However, unlike for boscalid and penconazole, transformation processes predominated for metazachlor, as demonstrated by the measurement of its

35 TPs. The low recoveries obtained for boscalid and penconazole after the flushings may be explained by their low leaching potential (USEPA, 2003; European Food Safety Authority (EFSA), 2008; Marín-Benito et al., 2015). As for the tracers, Br recovery was the highest, as expected given its most conservative character. The lowest recoveries of UR were assumed to be due to both retention and especially degradation, as already reported by Lange et al. (2018). Whereas SRB mainly experienced sorption, as evidenced by its behavior in the pore water and the results of the cumulative recovery curves.

40 ### 3.4 Final mass balance

The overall mass balance performed at the end of the experiment is shown in Fig. 8. According to the results, Br was recovered almost fully (98.3 %), while UR and SRB displayed lower recoveries (32.4 % and 76 %, respectively). Based on the different compartments, Br showed the highest recoveries in the outlet water, followed by the stems and leaves, whereas SRB and UR were mainly found in the sediment and the outlet water, respectively. These results highlighted different dissipation pathways

5 of the solutes. Indeed, as already evidenced by the breakthrough and cumulative recovery curves, Br displayed the most conservative character, although plant uptake was proven to be an important dissipation pathway for this tracer. In contrast, the main dissipation pathway of SRB was sorption, which was in agreement with its sorptive character (Kasnavia et al., 1999). UR, on the other hand, displayed comparatively lower recoveries, and based on the small amounts found in the sediments, sorption processes were not relevant for its dissipation. Thus, it is most likely that degradation via (bio-)chemical transformation was

10 the dominant process for UR, as already reported in other long-term studies (Maillard et al., 2016; Lange et al., 2018, Fernández-Pascual et al., 2018). Likewise, biochemical transformation contributed to metazachlor dissipation, as was confirmed by the measurements of its TPs, whereas the transformation of boscalid and penconazole could not be proven. Yet, it was not ruled out in the present study since the concentration of their metabolites may have been below the limit of quantification (≤ 9.29 and ≤ 10.28 µg L^{-1} for p-Chlorobenzoic acid and 1,2,4-Triazole, respectively). However, considering the duration of the

15 experiment (two months each run) and the DT$_{50}$ values of boscalid and penconazole, it was most likely that transformation did not take place. In addition, their high sorption affinity probably made them less bioavailable. Therefore, and based on the overall results, sorption played the main role in the dissipation of boscalid and penconazole. As for the plant uptake of pesticides, although it was not possible to measure it in the present study, it was assumed that it took place during the experiment. Previous investigations have already reported plant uptake of pesticides. For instance, Papaevangelou et al. (2017)

20 demonstrated that high amounts of boscalid accumulated in the tissue of *Phragmites australis* in constructed wetlands, although adsorption accounted as a main process as well. The same plant species was shown to take up, translocate and metabolize tebuconazole (Lv et al., 2017), a triazole fungicide similar to penconazole. Traces of metazachlor and its metabolites were also detected in the roots and stems of *Glyceria maxima* in wetland mesocosms experiments (Chen et al., 2017), although plant uptake was reported to play a negligible role in their removal.

25 The contribution of vegetation to uptake and breakdown was also confirmed by the final mass balance. Indeed, lower amounts of UR and Br were recovered from the pore water of the vegetated compared to the non-vegetated zone (Fig. 8A). Moreover, most of the TPs of metazachlor were recovered from the pore water of the vegetated zone. Contrary to expectations, the largest amounts of pesticides and SRB were recovered from the pore water of the vegetated zone. Yet, these results supported the hypothesis of the creation of preferential flow paths induced by the plants (Durst et al., 2013). On the other hand, most of SRB

30 was found sorbed in the sediment of the vegetated zone, where the highest concentration of organic carbon was located (Fig. 9), thereby contradicting the greatest tendency of SRB to sorption onto mineral surfaces (Kasnavia et al., 1999). Nevertheless, it has been recently demonstrated that SRB has high sorption affinity for litters in wetlands (Dollinger et al., 2017). Thus, probably the presence of dead leaves and decaying plant residues in the uppermost layer enhanced sorption of SRB.

4 Conclusions

35 The use of hydrological tracers with different sorptive and reactive properties together with selected pesticides and coupled with high vertical-resolution sampling and monitoring in a model constructed wetland system provided valuable information about transport and dissipation processes on a long-term basis and detailed spatial scale. By comparing tracers with selected pesticides, dominant transport vectors and main dissipation pathways could be identified.

Preferential flow was a crucial component affecting the fate and dissipation of solutes in the system and was caused by both

40 the constructional design of the inflow and the free water at the surface along with the plants. The strong positive correlation found between Br, UR and metazachlor highlighted the predominance of transport processes for these compounds. By contrast, SRB, boscalid and penconazole only displayed significant correlations where preferential flow paths took place, which, together

with their absence or low detection in the middle sediment layers suggested high sorption affinity. These findings were supported by the gradual increase in accumulated mass recovery obtained for these solutes during flushings. Yet, their different final recoveries indicated lower leaching potential of boscalid and penconazole compared to SRB.

The final overall mass balance indicated that plant uptake, transformation and sorption were the main dissipation pathways. The detection of metazachlor TPs, namely met-ESA and met-OA demonstrated that biochemical transformation had a major contribution to metazachlor dissipation. Met-ESA and met-OA recoveries obtained at the outlet of the system during flushings confirmed their great mobility and persistence. In contrast, sorption was the main dissipation pathway for boscalid and penconazole, although their transformation could not be ruled out within the timeframe of the present study. Likewise, plant uptake of pesticides could not be confirmed but was assumed to have taken place throughout the experiment.

Our findings pointed out that the alternation of different hydrological conditions (saturation and drying periods) favored the transformation of certain pesticides. Maximum relative concentrations of metazachlor TPs were measured after the promotion of aerobic conditions during the drying period. Similarly, the presence of plants was a key factor in boosting transformation processes, as evidenced by the increased occurrence of metazachlor TPs in the vegetated zone. Our study also revealed a different performance of the vegetated zone over time. In this case, unlike the non-vegetated, the vegetated zone did not show any correlation between the breakthrough curves of Br for each experimental run. This result was explained by possible changes in root density and/or spatial distribution during the experiment. As a result, different transport vectors and plant uptake rates took place in each experimental run.

Overall, the complexity of the processes that take place in buffer zones, such as constructed wetlands, and the lack of sufficient data on a temporal and spatial scale highlights the need to adopt new methods and perform further experiments, especially under field conditions combined with mathematical modeling. In this regard, the application of a multi-tracer approach coupled with high vertical-resolution sampling and monitoring may assist in unveiling internal mechanisms that dominate transport vectors and dissipation of contaminants in buffer zones.

Acknowledgements

This research has been carried out in the framework of the MUTReWa-project (02WRM1366B) funded by the German Federal Ministry for Education and Research. The authors wish to acknowledge Emil Blattmann and Britta Kattenstroth for their help with the construction of the experimental setup as well as Barbara Herbstritt, Jens Robertson, Felix Zimmermann and Maria Martin Pérez for sampling and analytical support. We would also like to thank Christine Stumpp for her valuable advice and contribution to the design of the sampling setup.

References

Aga, D. S., Thurman, E. M., Yockel, M. E., Zimmerman, L. R., & Williams, T. D.: Identification of a new sulfonic acid metabolite of metolachlor in soil, Environmental science & technology, 30(2), 592-597, 1996.

Aislabie, J., & Lloyd-Jones, G.: A review of bacterial-degradation of pesticides, Soil Research, 33(6), 925-942, 1995.

Bard, A.J., Parsons, R., Jordan, J.: Standard Potentials in Aqueous Solution. Marcel Dekker Inc., New York, 1985.

Birkigt, J., Stumpp, C., Małoszewski, P., & Nijenhuis, I.: Evaluation of the hydrological flow paths in a gravel bed filter modeling a horizontal subsurface flow wetland by using a multi-tracer experiment, Science of The Total Environment, 621, 265-272, 2018.

Bouldin, J. L., Farris, J. L., Moore, M. T., Smith Jr, S., Stephens, W. W., & Cooper, C. M.: Evaluated fate and effects of atrazine and lambda-cyhalothrin in vegetated and unvegetated microcosms, Environmental Toxicology: An International Journal, 20(5), 487-498, 2005.

Brix, H.: Do macrophytes play a role in constructed treatment wetlands?, Water science and technology, 35(5), 11-17, 1997.

5 Calderbank, A.: The occurrence and significance of bound pesticide residues in soil, in: Reviews of environmental contamination and toxicology (pp. 71-103). Springer, New York, NY, 1989.

Chen, Z., Chen, Y., Vymazal, J., Kule, L., & Koželuh, M.: Dynamics of chloroacetanilide herbicides in various types of mesocosm wetlands, Science of the Total Environment, 577, 386-394, 2017.

Dollinger, J., Dagès, C., & Voltz, M.: Using fluorescent dyes as proxies to study herbicide removal by sorption in buffer zones,
10 Environmental Science and Pollution Research, 24(12), 11752-11763, 2017.

Đurović, R., Gajić-Umiljendić, J., & Đorđević, T.: Effects of organic matter and clay content in soil on pesticide adsorption processes, Pesticidi i fitomedicina, 24(1), 51-57, 2009.

Durst, R., Imfeld, G., & Lange, J.: Transport of pesticides and artificial tracers in vertical-flow lab-scale wetlands, Water Resources Research, 49(1), 554-564, 2013.

15 Ebert, D., & Harder, U.: Boscalid: The degradation behaviour of 14C-BAS 510 F in different soils (DT50/DT90), BASF AG, Agrarzentrum Limburgerhof, 2000.

Edwards, C. A.: Factors that affect the persistence of pesticides in plants and soils, in: Pesticide Chemistry–3 (pp. 39-56), 1975.

European Food Safety Authority (EFSA).: Conclusion regarding the peer review of the pesticide risk assessment of the active substance metazachlor, EFSA Journal, 6(7), 145r, 2008.

20 European Food Safety Authority (EFSA).: Conclusion regarding the peer review of the pesticide risk assessment of the active substance penconazole, EFSA Journal, 6(10), 175r, 2008.

Eurostat: Agri-environmental indicator-pesticide pollution of water, Statistics explained, European Commission, https://ec.europa.eu/eurostat/statistics-explained/index.php/Archive:Agri-environmental_indicator_-_pesticide_pollution_of_water, 2012.

25 Fan, J., Zhang, B., Zhang, J., Ngo, H. H., Guo, W., Liu, F., ... & Wu, H.: Intermittent aeration strategy to enhance organics and nitrogen removal in subsurface flow constructed wetlands, Bioresource technology, 141, 117-122, 2013.

Fernández-Pascual, E., Zaman, S., Bork, M., Lang, F., & Lange, J.: Long-term mesocosm experiments to investigate degradation of fluorescent tracers. Journal of Hydrology X, 100014, 2018.

Flury, M., & Wai, N. N.: Dyes as tracers for vadose zone hydrology. Reviews of Geophysics, 41(1), 2003.

30 Goss, M. J., Miller, M. H., Bailey, L. D., & Grant, C. A.: Root growth and distribution in relation to nutrient availability and uptake, European Journal of Agronomy, 2(2), 57-67, 1993.

Gregoire, C., Elsaesser, D., Huguenot, D., Lange, J., Lebeau, T., Merli, A., ... & Schulz, R.: Mitigation of agricultural nonpoint-source pesticide pollution in artificial wetland ecosystems–a review, in: Climate Change, Intercropping, Pest Control and Beneficial Microorganisms, 293-338, Springer, Dordrecht, 2009.

35 Gutowski, L., Olsson, O., Lange, J., & Kümmerer, K.: Photolytic transformation products and biological stability of the hydrological tracer Uranine. Science of the Total Environment, 533, 446-453, 2015.

Hofmann, K.: Wachstumsverhalten von Schilf (Phragmites australis (Cav.) Trin. ex Steudel), in: klärschlammbeschickten Filterbeeten, Archiv für Hydrobiologie, 107(3), 385-409, 1986.

Käss, W., Behrens, H., & Behrens, H.: Tracing technique in geohydrology, Rotterdam: Balkema, 581, 1998.

Karlsson, A. S., Weihermüller, L., Tappe, W., Mukherjee, S., & Spielvogel, S.: Field scale boscalid residues and dissipation half-life estimation in a sandy soil, Chemosphere, 145, 163-173, 2016.

Kasnavia, T., Vu, D., & Sabatini, D. A.: Fluorescent dye and media properties affecting sorption and tracer selection, Ground water, 37(3), 376-381, 1999.

Kolpin, D. W., Schnoebelen, D. J., & Thurman, E. M.: Degradates provide insight to spatial and temporal trends of herbicides in ground water, Groundwater, 42(4), 601-608, 2004.

Lange, J., Schuetz, T., Gregoire, C., Elsässer, D., Schulz, R., Passeport, E., & Tournebize, J.: Multi-tracer experiments to characterise contaminant mitigation capacities for different types of artificial wetlands, International Journal of Environmental and Analytical Chemistry, 91(7-8), 768-785, 2011.

Lange, J., Olsson, O., Sweeney, B., Herbstritt, B., Reich, M., Alvarez-Zaldivar, P., ... & Imfeld, G.: Fluorescent tracers to evaluate pesticide dissipation and transformation in agricultural soils, Science of The Total Environment, 619, 1682-1689, 2018.

Leibundgut, C., Maloszewski, P., & Külls, C.: Environmental tracers. Tracers in Hydrology, John Wiley & Sons, Ltd., Chichester, UK, 13-56, 2009.

Long, R., Gan, J., & Nett, M.: Pesticide choice: Best management practice (BMP) for protecting surface water quality in agriculture, 2005.

Lv, T., Carvalho, P. N., Bollmann, U. E., Arias, C. A., Brix, H., & Bester, K.: Enantioselective uptake, translocation and degradation of the chiral pesticides tebuconazole and imazalil by Phragmites australis, Environmental pollution, 229, 362-370, 2017.

Maillard, E., Payraudeau, S., Faivre, E., Grégoire, C., Gangloff, S., & Imfeld, G.: Removal of pesticide mixtures in a stormwater wetland collecting runoff from a vineyard catchment, Science of the Total Environment, 409(11), 2317-2324, 2011.

Maillard, E., Lange, J., Schreiber, S., Dollinger, J., Herbstritt, B., Millet, M., & Imfeld, G.: Dissipation of hydrological tracers and the herbicide S-metolachlor in batch and continuous-flow wetlands, Chemosphere, 144, 2489-2496, 2016.

Mamy, L., Barriuso, E., & Gabrielle, B.: Environmental fate of herbicides trifluralin, metazachlor, metamitron and sulcotrione compared with that of glyphosate, a substitute broad spectrum herbicide for different glyphosate-resistant crops, Pest Management Science: formerly Pesticide Science, 61(9), 905-916, 2005.

Martin, A., Margoum, C., Jolivet, A., Assoumani, A., El Moujahid, B., Randon, J., & Coquery, M.: Calibration of silicone rubber rods as passive samplers for pesticides at two different flow velocities: Modeling of sampling rates under water boundary layer and polymer control, Environmental toxicology and chemistry, 37(4), 1208-1218, 2018.

Marín-Benito, J. M., Rodríguez-Cruz, M. S., Sánchez-Martín, M. J., & Mamy, L.: Modeling fungicides mobility in undisturbed vineyard soil cores unamended and amended with spent mushroom substrates, Chemosphere, 134, 408-416, 2015.

McMahon, P. B., Dennehy, K. F., Michel, R. L., Sophocleous, M. A., Ellett, K. M., & Hurlbut, D. B.: Water movement through thick unsaturated zones overlying the central High Plains aquifer, southwestern Kansas, 2000–2001, USGS Water Resources Investigation Report, 3(4171), 32, 2003.

Mehra, O. P., & Jackson, M. L.: Iron oxide removal from soils and clays by a dithionite–citrate system buffered with sodium bicarbonate, in: Clays and clay minerals: proceedings of the Seventh National Conference, 317-327, 1960.

Müller, K., Bach, M., Hartmann, H., Spiteller, M., & Frede, H. G.: Point-and nonpoint-source pesticide contamination in the Zwester Ohm catchment, Germany, Journal of environmental quality, 31(1), 309-318, 2002.

5 Ong, S. A., Uchiyama, K., Inadama, D., Ishida, Y., & Yamagiwa, K.: Performance evaluation of laboratory scale up-flow constructed wetlands with different designs and emergent plants, Bioresource technology, 101(19), 7239-7244, 2010.

Papaevangelou, V. A., Gikas, G. D., Vryzas, Z., & Tsihrintzis, V. A.: Treatment of agricultural equipment rinsing water containing a fungicide in pilot-scale horizontal subsurface flow constructed wetlands, Ecological engineering, 101, 193-200, 2017.

10 Passeport, E., Tournebize, J., Jankowfsky, S., Prömse, B., Chaumont, C., Coquet, Y., & Lange, J.: Artificial wetland and forest buffer zone: hydraulic and tracer characterization, Vadose Zone Journal, 9(1), 73-84, 2010.

Petticrew, E. L., & Kalff, J.: Water flow and clay retention in submerged macrophyte beds, Canadian Journal of Fisheries and Aquatic Sciences, 49(12), 2483-2489, 1992.

Reemtsma, T., Alder, L., & Banasiak, U.: Emerging pesticide metabolites in groundwater and surface water as determined by
15 the application of a multimethod for 150 pesticide metabolites, Water research, 47(15), 5535-5545, 2013.

Rose, M. T., Crossan, A. N., & Kennedy, I. R.: The effect of vegetation on pesticide dissipation from ponded treatment wetlands: Quantification using a simple model, Chemosphere, 72(7), 999-1005, 2008.

Sabatini, D. A.: Sorption and intraparticle diffusion of fluorescent dyes with consolidated aquifer media, Groundwater, 38(5), 651-656, 2000.

20 Sanchez-Martin, M. J., Andrades, M. S., & Sánchez-Camazano, M.: Soil properties influencing the adsorption and mobility of penconazole in vineyard soils, Soil science, 165(12), 951-960, 2000.

Sannino, F., Filazzola, M. T., Violante, A., & Gianfreda, L.: Fate of herbicides influenced by biotic and abiotic interactions, Chemosphere, 39(2), 333-341, 1999.

Smart, P. L., & Laidlaw, I. M. S.: An evaluation of some fluorescent dyes for water tracing, Water Resources Research, 13(1),
25 15-33, 1977.

Stang, C., Wieczorek, M. V., Noss, C., Lorke, A., Scherr, F., Goerlitz, G., & Schulz, R.: Role of submerged vegetation in the retention processes of three plant protection products in flow-through stream mesocosms, Chemosphere, 107, 13-22, 2014.

Stehle, S., & Schulz, R.: Agricultural insecticides threaten surface waters at the global scale, Proceedings of the National Academy of Sciences, 112(18), 5750-5755, 2015.

30 Torrentó, C., Prasuhn, V., Spiess, E., Ponsin, V., Melsbach, A., Lihl, C., ... & Hunkeler, D.: Adsorbing vs. nonadsorbing tracers for assessing pesticide transport in arable soils, Vadose Zone Journal, 2017.

University of Hertfordshire, PPDB: Pesticide properties database, 2010.

USEPA (US Environmental Protection Agency), Pesticide Fact Sheet, Boscalid, 2003.

Vallée, R., Dousset, S., Billet, D., & Benoit, M.: Sorption of selected pesticides on soils, sediment and straw from a constructed
35 agricultural drainage ditch or pond, Environmental Science and Pollution Research, 21(7), 4895-4905, 2014.

Vorenhout, M., van der Geest, H. G., & Hunting, E. R.: An improved datalogger and novel probes for continuous redox measurements in wetlands, International Journal of Environmental and Analytical Chemistry, 91(7-8), 801-810, 2011.

Vymazal, J.: Horizontal sub-surface flow and hybrid constructed wetlands systems for wastewater treatment, Ecological engineering, 25(5), 478-490, 2005.

Vymazal, J., & Březinová, T.: The use of constructed wetlands for removal of pesticides from agricultural runoff and drainage: a review, Environment international, 75, 11-20, 2015.

5   Wernli, H. R.: Einführung in die Tracerhydrologie: hydrologisches Praktikum, Geographisches Institut Univ. Bern, 2009.

Whitmer, S., Baker, L., & Wass, R.: Loss of bromide in a wetland tracer experiment, Journal of Environmental Quality, 29(6), 2043-2045, 2000.

Włodarczyk, M.: Influence of formulation on mobility of metazachlor in soil, Environmental monitoring and assessment, 186(6), 3503-3509, 2014.

10   **Figures**
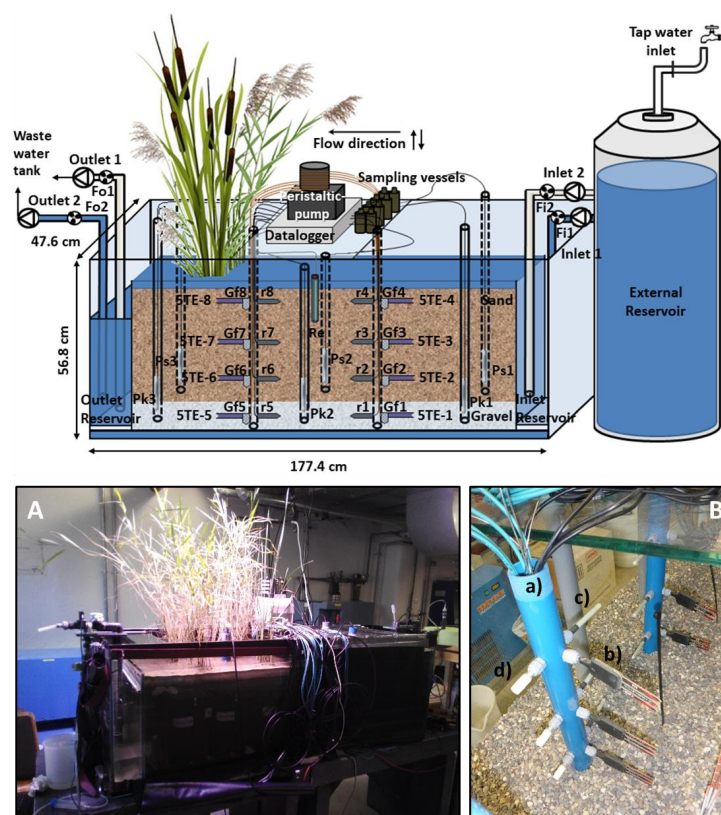
Figure 1: Schematic representation of the model constructed wetland system (not to scale).

Fi1 and Fi2 indicate the flowmeters at the inlet; Fo1 and Fo2, the flowmeters at the outlet; Ps(n), piezometer in the sand; Pk(n), piezometer in the gravel; 5TE-(n), soil moisture, temperature and electrical conductivity sensor; r(n), platinum redox electrode; Re, reference electrode (Ag:AgCl); Gf(n), glassfilter. For the piezometers, n indicates the position with respect to the inlet; n=1, close to the inlet; n=2, in the middle of the sediment bed and n=3, close to the outlet. For the sensors installed in the multi-level pipes, n indicates the zone and the depths where they are located; n = 1, 2, 3 and 4, non-vegetated zone at a depth of 39, 27, 15 and 3 cm, respectively; n = 5, 6, 7 and 8, vegetated zone at a depth of 39, 27, 15 and 3 cm, respectively.

(A) front view photograph of the model constructed wetland system; (B) detail of the multi-level pipes: (a) multi-level pipe at the
20   **vegetated zone, (b) 5TE sensor, (c) redox electrode and (d) glass filter.**
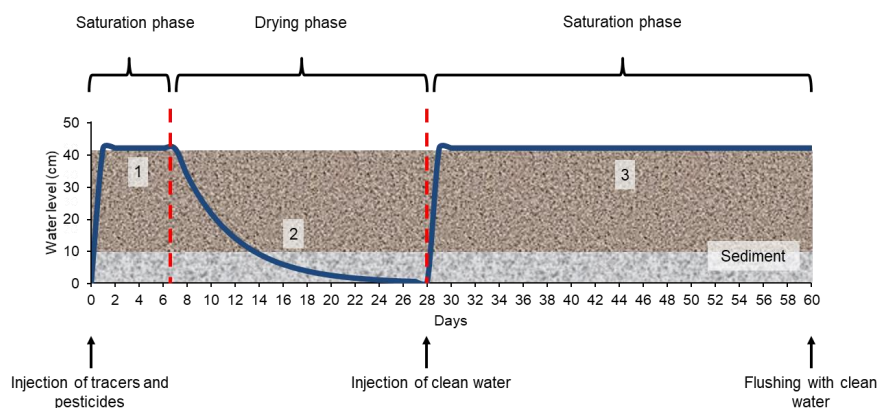
Figure 2: Experimental protocol with the different phases and injections performed during the experiment. The x-axis indicates the duration of the experiment and the y-axis the variation of the water level during the different phases.

5 **Note Fig. 2: The water level curve (blue) is only schematic and does not correspond to real water level measurements.**
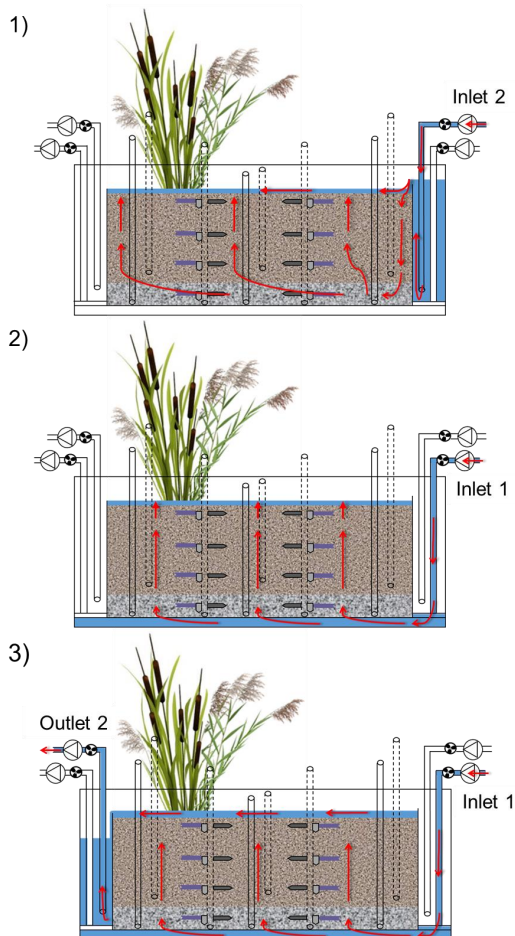
Figure 3: Front view of the model constructed wetland system showing the execution of the injections (red arrows indicate the direction of water flow): (1) surface injection of tracers and pesticides, (2) injection of clean water (tap water) from the bottom, (3) flushing of the system with clean water (tap water) from the bottom.
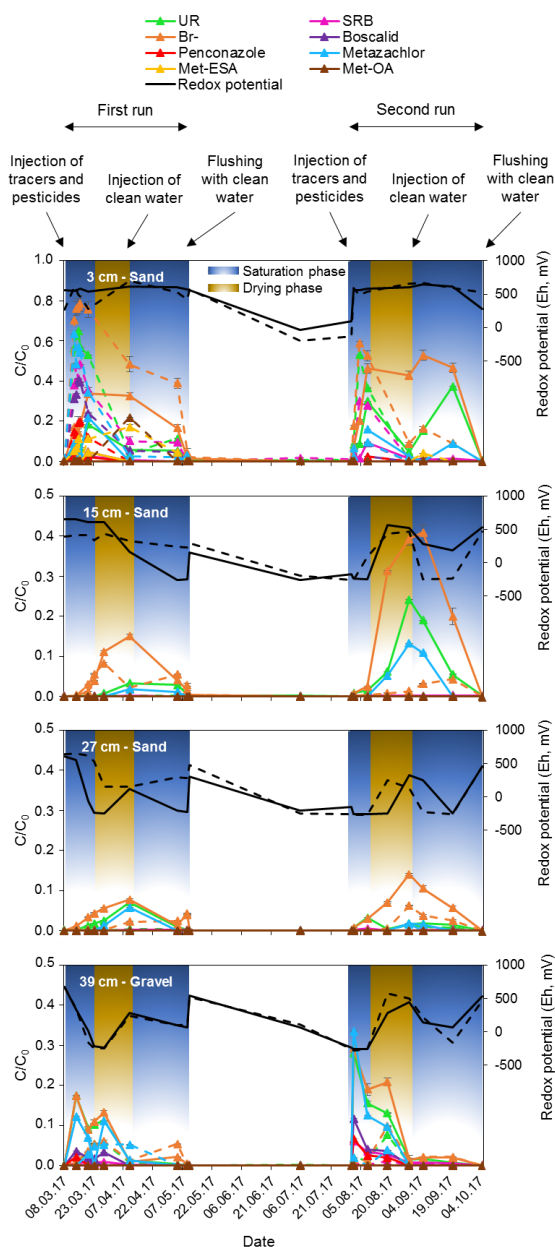
Figure 4: Breakthrough curves of the different tracers, pesticides and their TPs in terms of relative concentrations (C/C₀) (obtained by scaling with the input concentrations) measured in the pore water during each run at different depths and phases (saturation and drying). Changes in redox potential are displayed in the second y-axis (Eh in mV). For both, the relative concentration and the redox potential, the solid lines represent the values measured in the non-vegetated zone and the dashed lines the values measured in the vegetated zone. The different injections performed during each run are displayed on top of the figure. Note that the scale of the relative concentrations corresponding to the sampling depth of 3 cm is extended.
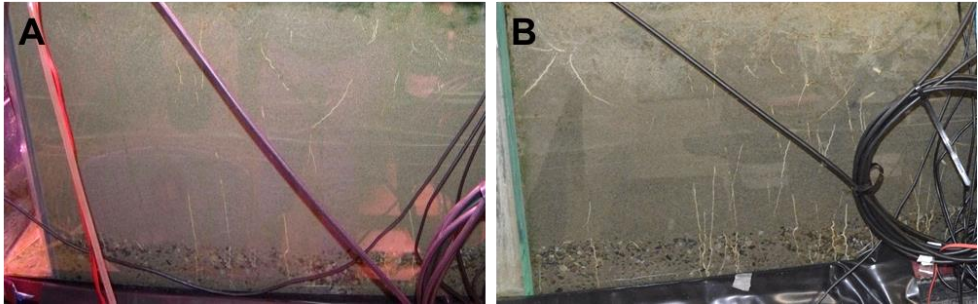
Figure 5: Front view photograph of the root system in the vegetated part of the model constructed wetland for: A) before the first run and B) at the end of the second run.
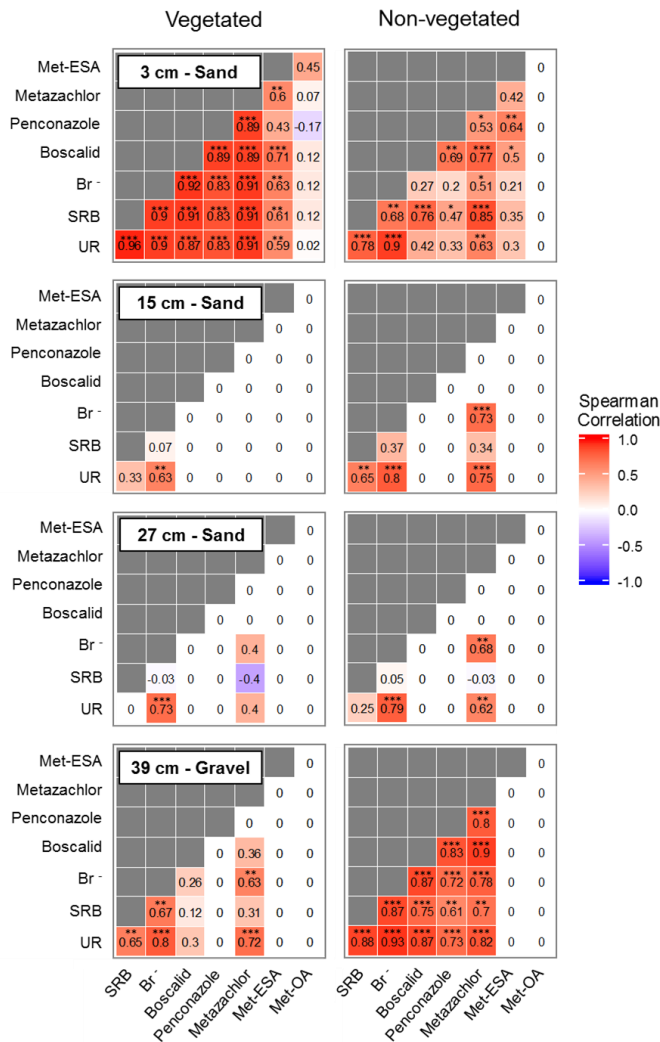
5 **Figure 6: Spearman correlation matrices between the relative concentration of tracers, pesticides and their TPs in the pore water during the whole experiment, distinguishing between the different depths and zones.**

Signif. Codes: 0.001 '*'; 0.01 '**'; 0.05 '*'**
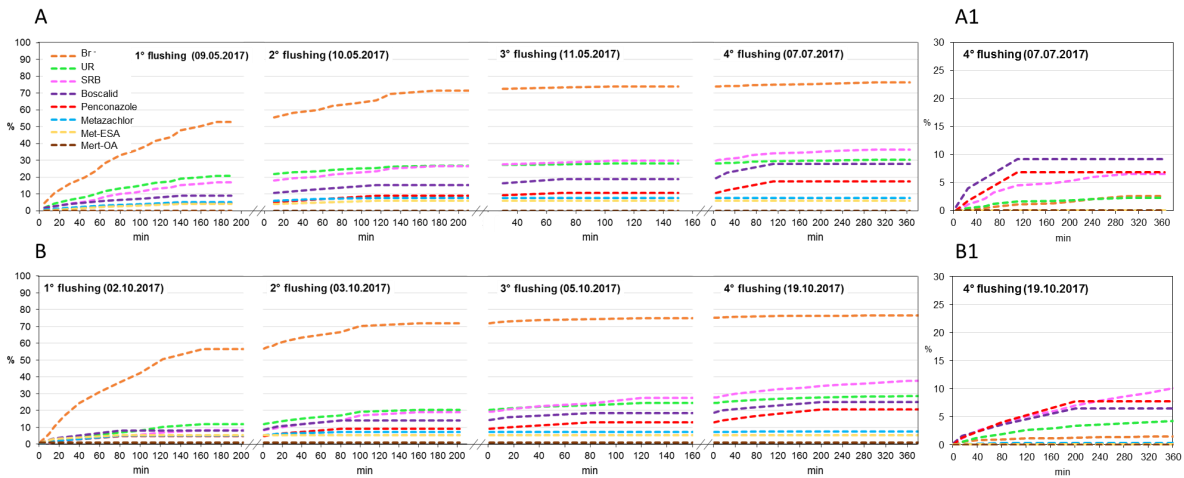
Figure 7: Cumulative recovery curves of tracers, pesticides and their TPs during the four flushings for: A) first and B) second run. Recovery curves for the fourth flushing are detailed in: A1 and B1 for the first and the second run, respectively.

Recoveries of tracers, pesticides and their TPs at the outlet
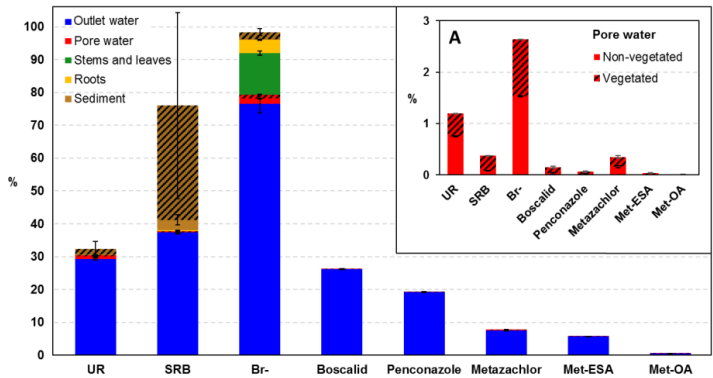
5 **Figure 8: Final mass balance conducted at the end of the experiment in the different compartments.**

Note that the pesticides and their TPs could only be measured in the outlet and pore water compartments. The shaded area represents the percentage measured in the vegetated zone. The mass balance for the pore water compartment is detailed in the upper right portion of the graph (A).
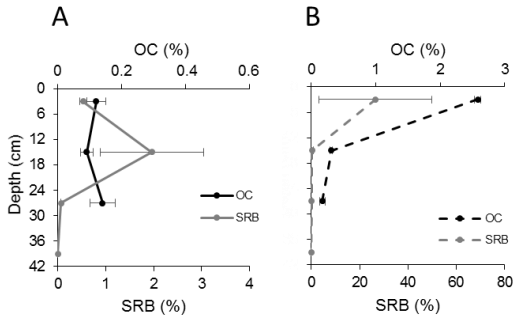
10 **Figure 9: Selected vertical gradients of percentage of organic carbon content (OC) and SRB measured in the sediment at the end of the experiment for A) non-vegetated and B) vegetated zone. Values represent means of duplicates ± standard deviation.**

Tables

Table 1: Physico-chemical properties of the applied tracers and pesticides (20°C-25°C).

Property	Unit	UR	SRB	Br	Boscalid	Penconazole	Metazachlor
Chemical formula		$C_{20}H_{10}O_5Na_2$	$C_{27}H_{29}N_2NaO_7S_2$	NaBr	$C_{18}H_{12}Cl_2N_2O$	$C_{13}H_{15}Cl_2N_3$	$C_{14}H_{16}ClN_3O$
Chemical family		Xanthene dye	Xanthene dye	Inorganic salt	Carboxamide	Triazole	Chloroacetamide
Molecular mass [a]	g mol^{-1}	376.3	580.7	102.9	342.0	283.1	277.1
Aqueous solubility	g L^{-1}	25.0[b]	70.0[b]	850[c]	0.0046[d]	0.073[d]	0.450[d]
Aqueous diffusion coefficient	cm[2] s	3.5 x 10[-6c]	4.7 x 10[-6c]	-	4.4 x 10[-12g]	-	-
Soil degradation (DT50) typical	days	-	-	stable[c]	200[d] (persistent)	117[d] (persistent)	8.6[d] (non-persistent)
Dissipation rate on plant matrix (RL50)	days	-	-	-	6.9[d]	65.6[d]	-
Photolytic stability (DT50)	days	0.5[c]	34[c]	stable[c]	30[d] (stable)	4[d] (moderately fast)	stable[d]
Hydrolytic stability (DT50)	days	stable[c]	stable[c]	stable[c]	stable[d]	stable[d]	stable[d]
Water-sediment (DT50)	days	stable[i]	stable[i]	-	-	853[d] (stable)	20.6[d] (fast)
Organic carbon - water partitioning (Koc)	L kg^{-1}	0-62[b]	147-498[b]	-	772.0[f]	2205[f]	134.0[f]
Octanol - water partitioning (Log Kow) at pH 7		1.26-3.56[h]	0.21-4.77[h]	-	2.96[d]	3.72[d]	2.49[d]
GUS leaching potential index		-	-	-	2.66[d] (transition state)	1.36[d] (low)	2.17[d] (transition state)

[-] Information not available
[a] From ChemID database (2017)
[b] From Sabatini (2000)
[c] From Leibundgut et al. (2009)
[d] From Pesticide Properties DataBase, University of Hertfordshire.
[e] From Merck Millipore (http://www.merckmillipore.de)
[f] From PAN Pesticides Database (.pesticideinfo.org/Search_Chemicals.jsp)
[g] From Martin et al. (2017)
[h] From EPA Chemistry Dashboard
[i] From Smart and Laidlaw (1977)

Table 2: (A) characteristics and (B) operation of the model constructed wetland system.

A

Compartment	Parameter	Unit	sub-compartment	Value
Sediments	Texture*	% Sand/Silt/Clay	Sand	97.8/2.3/0.1
	Mean initial organic carbon content *	%	Sand	0.2 ± 0.0
	Mean final organic carbon content **	%	Sand	0.8 ± 1.4
	Mean initial dithionite-extractable Fe (Fed)*	g Kg[-1]	Sand	1.0 ± 0.0
	Mean final dithionite-extractable Fe (Fed)**	g Kg[-1]	Sand	1.1 ± 0.2
	pH (H_2O)	-	Sand	9.1
	pH ($CaCl_2$)	-	Sand	8.1
	Diameter*	mm	Sand	0-2
			Gravel	4-8
	Bulk density*	Kg L[-1]	Sand	1.5
			Gravel	1.6
	Porosity	%	Sand	42
			Gravel	45
	Height	cm	Sand	32
			Gravel	10
	Surface area	m[2]	-	0.7
	Mass	Kg	Sand	430.8

			Gravel	124.0
Plants	Density	N°	*Typha latifolia*	4
			Phragmites australis	7
		Plants m⁻²	*Typha latifolia*	10.8
			Phragmites australis	18.9
	Mean initial height	cm	*Typha latifolia*	79.8 ± 18.6
			Phragmites australis	76.9 ± 10.1

* Determined prior to planting
** Determined at the end of the experiment as the mean of all the values measured at the different depths

B

Parameter	Unit	Value
Inlet/outlet pumping rate	L h⁻¹	21.6
Peristaltic pumping rate	L h⁻¹	0.1
Volume of tracers and pesticides solution injected	L	40
Volume of clean water injected at the end of the drying phase	L	34.1 ± 3.1
Volume of total clean water injected in the flushings	L	355.1 ± 20.5

Values represent means ± standard deviation

Table 3: Spearman rank correlation between the breakthrough curves of Br of the first and the second experimental run, distinguishing between the different depths and zones.

Depth (cm)	Zone	rho	p-value
3	Non-vegetated	0.29	0.56
	Vegetated	0.14	0.80
15	Non-vegetated	0.84	<0.01 **
	Vegetated	0.55	0.17
27	Non-vegetated	0.77	0.03 *
	Vegetated	0.26	0.53
39	Non-vegetated	0.73	0.04 *
	Vegetated	0.55	0.15

Signif. Codes: 0.001 '***'; 0.01 '**'; 0.05 '*'

Table 4: Percentage of total bromide recovered from the pore water for the first and second run, distinguishing between the different depths and zones.

Depth (cm)	Zone	Recovery pore water (%) 1° run	Recovery pore water (%) 2° run	Mean recovery (%)
3	Non-vegetated	0.6	0.7	0.6 ± 0.1
	Vegetated	1.3	0.4	0.8 ± 0.7
15	Non-vegetated	0.3	0.5	0.4 ± 0.1
	Vegetated	0.2	0.1	0.1 ± 0.1
27	Non-vegetated	0.2	0.2	0.2 ± 0
	Vegetated	0.1	0.1	0.1 ± 0
39	Non-vegetated	0.4	0.3	0.3 ± 0.1
	Vegetated	0.1	0.1	0.1 ± 0

Mean recovery represents means ± standard deviation.

Table 5: Percentage of tracers, pesticides and their TPs recovered from the outlet water after the flushings of the system for the first and second run.

	Recovery water outlet (%) 1° run	Recovery water outlet (%) 2° run	Mean recovery (%)
Br	76.5	76.7	76.6 ± 0.1
UR	30.3	28.8	29.6 ± 1.1
SRB	36.4	38.0	37.2 ± 1.1
Boscalid	27.9	24.9	26.4 ± 2.1
Penconazole	17.3	20.7	19.0 ± 2.4
Metazachlor	7.5	7.4	7.5 ± 0.1
Met-ESA	6.1	5.4	5.8 ± 0.5
Met-OA	0	0.8	0.4 ± 0.6

Mean recovery represents means ± standard deviation.